MOLECULAR IMAGING AND BIOLOGY

Mol Imaging Biol (2016) 18:201–208
DOI: 10.1007/s11307-015-0876-y

Published Online: 5 August 2015

RESEARCH ARTICLE

Predicting Response to Therapy for Autoimmune and Inflammatory Diseases Using a Folate Receptor-Targeted Near-Infrared Fluorescent Imaging Agent

Lindsay E. Kelderhouse, Sakkarapalayam Mahalingam, Philip S. Low

Department of Chemistry, Purdue University, 720 Clinic Drive, West Lafayette, IN, 47907, USA

Abstract

Purpose: Although current therapies for many inflammatory/autoimmune diseases are effective, a significant number of patients still exhibit only partial or negligible responses to therapeutic intervention. Since prolonged use of an inadequate therapy can result in both progressive tissue damage and unnecessary expense, methods to identify nonresponding patients are necessary.
Procedures: Four murine models of inflammatory disease (rheumatoid arthritis, ulcerative colitis, pulmonary fibrosis, and atherosclerosis) were induced, treated with anti-inflammatory agents, and evaluated for inflammatory response. The mice were also injected intraperitoneally with OTL0038, a folate receptor-targeted near-infrared dye that accumulates in activated macrophages at sites of inflammation. Uptake of OTL0038 in inflamed lesions was then correlated with clinical measurements of disease severity.
Results: OTL0038 accumulated at sites of inflammation in all four animal models. More importantly, changes in lesion-associated OTL0038 preceded changes in clinical symptoms in mice treated with all anti-inflammatory drugs examined.
Conclusion: OTL0038 has the ability to predict responses to multiple therapies in four murine models of inflammation.

Key words: Inflammatory and autoimmune diseases, Folate receptor targeting, Activated macrophages, Near-infrared fluorescent dye, Fluorescence imaging of autoimmune disease, Idiopathic pulmonary fibrosis imaging, Rheumatoid arthritis imaging, Ulcerative colitis imaging, Atherosclerosis imaging

Introduction

Management of inflammatory and autoimmune diseases (rheumatoid arthritis, ulcerative colitis, atherosclerosis, psoriasis, ischemia/reperfusion injury, pulmonary fibrosis, organ transplant rejection, multiple sclerosis, scleroderma, Crohn's disease, Sjogren's syndrome, glomerulonephritis, sarcoidosis, etc.) is often complicated by an inability to predict a patient's response to any selected therapy [1–3]. While conventional strategies for assessing improvement in clinical symptoms (*i.e.*, changes in radiography, reduction in pain, improvement in coloration and/or swelling) are still widely used, significant changes in these parameters may only become apparent after months of therapy [4–8]. For nonresponding patients, such a delay in identification of an ineffective therapy can lead to irreversible damage and the passing of an ideal "window of therapeutic opportunity" [9,

Electronic supplementary material The online version of this article (doi:10.1007/s11307-015-0876-y) contains supplementary material, which is available to authorized users.

Correspondence to: Philip Low; *e-mail:* plow@purdue.edu

10]. Therefore, sensitive and specific methods are needed to detect the earliest changes in disease status so that the most effective therapy can quickly be administered.

Near-infrared (NIR) fluorescence imaging has attracted increased attention as a possible modality for *in vivo* monitoring of biologic processes, primarily because it is not compromised by damaging radiation, its fluorescent signal penetrates tissues to significant depths, its emission does not overlap with tissue autofluorescence, and it is essentially nontoxic at commonly used doses [11]. Indocyanine green (ICG), an FDA-approved NIR dye, for example, has been exploited to localize sentinel lymph nodes [12], identify inflamed joints [13, 14], assess liver function [15], determine cardiac output [16], and perform ophthalmic angiography [17] among many other applications. However, while ICG imaging has often proven adequate for detection of changes in inflamed lesions [13, 14], it still suffers from significant nonspecificity due to the fact that its accumulation at sites of inflammation depends primarily on enhanced vascular permeability and not on any tropism for inflammation markers. One obvious strategy for circumventing this lack of specificity would be to develop a ligand-targeted NIR probe that could selectively bind a receptor that is uniquely expressed on inflammatory cells and essentially absent from healthy tissues. In this article, we describe such an approach.

The beta isoform of the folate receptor (FR-β) is a glycosylphosphatidylinositol-anchored cell surface protein that binds folic acid with subnanomolar affinity and is uniquely overexpressed on activated macrophages [18, 19]. These FR-β^+ macrophages have been shown to constitute key players in the development and progression of a number of inflammatory and autoimmune diseases, and FR-targeted imaging agents have been exploited to visualize sites of activated macrophage accumulation in both animals and humans [20–24]. Importantly, uptake of FR-targeted imaging agents by activated macrophages has been found to correlate directly with severity of disease symptoms, indicating the potential use of FR-targeted imaging agents for monitoring autoimmune disease progression and response to therapy [25].

In this study, we demonstrate that accumulation of OTL0038 (a FR-targeted NIR dye) [26, 27] in the inflamed lesions of murine models of rheumatoid arthritis, ulcerative colitis, pulmonary fibrosis, and atherosclerosis shortly after initiation of therapy can accurately predict a subsequent response to all of the more common treatments for the above diseases; *i.e.*, long before clinical changes can be detected. Based on these studies, we suggest that OTL0038 and other folate receptor-targeted imaging agents could prove useful as clinical tools for the selection of those patients who will eventually benefit from treatment with a particular anti-inflammatory drug.

Methods

Animal Models

All animal procedures were approved by the Purdue Animal Care and Use Committee in accordance with guidelines from the National Institutes of Health. Mice were maintained in a temperature- and humidity-controlled room on a 12-h dark–light cycle with food and water available *ad libitum*.

Collagen-Induced Arthritis

Collagen-induced arthritis (CIA) was initiated using established methods on 6–7-week-old female DBA/1 mice (Jackson Laboratories) maintained on folate-deficient diet (Harlan-Teklad) [28]. Briefly, mice were immunized at the base of the tail with 100 μg bovine type II collagen emulsified in complete Freund's adjuvant (Chondrex, Inc., Redmond, WA, USA). Mice were then boosted 21 days later with a similar injection of 100 μg bovine type II collagen emulsified in incomplete Freund's adjuvant. After 4 days, onset of arthritis was synchronized with an intraperitoneal injection of 25 μg lipopolysaccharide (LPS) dissolved in saline. Three days later, mice were distributed randomly across control and treatment groups (n=5). Healthy mice and disease control mice received daily intraperitoneal injections of 100 μL saline. Diseased mice to be tested for response to therapy received daily intraperitoneal injections of dexamethasone (0.5 mg/kg) [29] or abatacept (300 μg) [30]. Arthritis scores were assessed every other day by researchers blinded to the various treatment groups, using the following scoring system: 0=normal; 1=mild, but definite redness and swelling of the ankle or wrist or apparent redness and swelling limited to individual digits, regardless of the number of affected digits; 2=moderate redness and swelling of ankle or wrist; 3=severe redness and swelling of the entire paw including digits; and 4=maximally inflamed limb with involvement of multiple joints. A total score for each mouse was calculated by summing the scores for each of the four paws, allowing a maximum possible score of 16 per animal. Paw thickness was measured with calipers every other day starting on the first day of treatment. On day 3 of treatment, mice were anesthetized with isoflurane and imaged for OTL0038 uptake as described below. Mice were again imaged after euthanasia by CO_2 asphyxiation on day 11 of treatment.

Ulcerative Colitis

Ulcerative colitis was induced as previously described [31]. Seven-week-old Balb/c mice (Harlan Laboratories) maintained on a folate-deficient diet were administered 5 % dextran sodium sulfate (DSS) in their drinking water. Healthy control mice were maintained on normal water. Mice were divided into treatment groups (n=10 per group). Healthy mice and disease control mice received 100 μl saline daily by oral gavage. Diseased mice to be tested for response to therapy were treated daily with cimetidine (100 mg/kg) [32] or sulfasalazine (150 mg/kg) [33] by oral gavage. Disease symptoms were assessed daily and quantitated by adding the scores from each of the following tests: weight loss: 0=no weight loss, 1=1–5 % weight loss, 2=6–10 % weight loss, 3=11–15 % weight loss, and 4=>15 % weight loss; stool appearance: 0=normal, 1=loose feces,

and 2=diarrhea; hematochezia (blood in stool): 0=no blood, 1=positive via guaiac paper, and 2=visually bloody; and overall appearance: 0=normal, 1=ruffled fur/altered gait, and 2=lethargic, moribund. On day 4 of therapy, half of each treatment group (n=5) received an intraperitoneal injection of 10 nmol OTL0038. After 4 h, the injected mice were euthanized, and colons were removed and measured with calipers to assess colon shortening and then immediately imaged for evaluation of OTL0038 accumulation. On day 10, the remaining mice were injected with OTL0038 and analyzed similarly.

Atherosclerosis

Five-week-old male *ApoE*−/− mice were purchased from Jackson Laboratories and placed on an adjusted calorie diet (42 % from fat, Harlan Laboratories) [34]. Healthy control mice (C57BL/6) were similarly maintained on normal chow. Mice were divided into therapy groups (n=5), and healthy mice and disease control mice received 100 µL saline daily by oral gavage. Diseased mice to be tested for response to therapy were treated daily with valsartan [35] (1 mg/kg) or fluvastatin (3 mg/kg) [36] by oral gavage. After 3 weeks of treatment, the mice had the black hair removed from their chest area and were imaged with OLT0038. Mice were again imaged with 10 nmol OTL0038 after 12 weeks of therapy and then euthanized by CO_2 asphyxiation. Aortas were dissected and submitted to the Purdue Histology and Phenotyping Laboratory for hematoxylin and eosin (H&E) staining.

Pulmonary Fibrosis

Pulmonary fibrosis was induced in mice as previously described [37]. Briefly, 6-week-old female C57BL/6 mice (Harlan Laboratories) maintained on a folate-deficient diet were anaesthetized with isoflurane, and 50 µl of bleomycin (2 U/kg body weight) dissolved in saline was intratracheally instilled into each mouse. Healthy control mice were similarly intratracheally instilled with 50 µl saline. Mice were then separated into treatment groups (n=5). Healthy mice and disease control mice received daily intraperitoneal injections of 100 µl saline. Diseased mice to be tested for response to treatment were injected every day intraperitoneally with dexamethasone (0.5 mg/kg) or etanercept (300 µg) [38]. Mice had the black hair removed from their chest and were imaged with OTL0038 after 6 days of treatment and again after 15 days of treatment. Mice were then euthanized by CO_2 asphyxiation, and bronchoalveolar lavage fluid was collected and component cells were counted with a Beckman Coulter Z™ Series Cell and Particle Counter. The left lung was fixed in formalin and submitted to the Purdue Histology and Phenotyping Laboratory for H&E staining, and the right lung was used for analysis of hydroxyproline content using a hydroxyproline assay kit from Sigma-Aldrich (St. Louis, MO).

Imaging of Sites of Macrophage Accumulation in Inflamed Mice with OTL0038

OTL0038, a folate-targeted NIR fluorescent dye with λex=776 nm and λem=794 nm, was synthesized as previously described [26, 27]. Ten nanomoles of OTL0038 was injected intraperitoneally into the desired mice, and unbound OTL0038 was allowed to clear from tissues for 4 h. Mice were then either anesthetized with 3 % isoflurane (CIA, atherosclerosis, and pulmonary fibrosis mice) or euthanized (ulcerative colitis mice) prior to image acquisition using a Kodak Imaging Station operated with Kodak molecular imaging version 4.5 software (atherosclerosis and pulmonary fibrosis) or a Caliper IVIS Lumina II Imaging Station with Living Image 4.0 software (rheumatoid arthritis and ulcerative colitis). Settings for white light imaging with the Kodak Imaging Station were as follows: illumination source=white light, acquisition time=0.175 s, f-stop=11, focal plane=5, field of view (FOV)=160, and binning=none. Settings for fluorescence images were as follows: illumination source=multiwavelength (755 nm), acquisition time=2 min, f-stop=2.80, focal plane=5, FOV=160, and binning=4 pixels. Settings for imaging with the Caliper IVIS Lumina II Imaging Station were as follows: lamp level, high; excitation, 745 nm; emission, ICG; binning, (M) 4; FOV=12.5; f-stop=4; and acquisition time=1 s.

Results

Analysis of Response to Therapy for Rheumatoid Arthritis with OTL0038

Due to the enhanced accumulation of FR^+ macrophages in inflamed lesions from patients with inflammatory/autoimmune diseases [20–24], we decided to evaluate the ability of OTL0038 (a FR-targeted NIR dye) to accurately predict patient response to therapy. For this purpose, mice were induced to develop collagen-induced arthritis (CIA) and subjected 28 days later to treatment with dexamethasone, abatacept, or saline (disease control). Three days after initiation of therapy, the mice were injected with 10 nmol OTL0038 and imaged 4 h later. As seen in Fig. 1a, mice induced to develop CIA but not treated with an anti-inflammatory drug exhibited high accumulation of OTL0038 in their inflamed appendages. However, inflamed mice injected with either dexamethasone or abatacept displayed markedly less OTL0038 uptake in the affected paws (Fig. 1a), despite revealing no reduction in disease symptoms (arthritis score, paw swelling) at this early time point (Fig. 1b, c). Moreover, after 11 days of continuous therapy, when the treated mice had finally responded to their respective therapies and joint inflammation had substantially subsided (Fig. 1b, c), images of the same mice (Supplemental Fig. 1) confirmed the significantly reduced uptake of OTL0038 in the treated mice relative to disease control mice. These data suggested that uptake of OTL0038 in the inflamed joints of CIA mice soon after initiation of therapy might predict an eventual response to a variety of therapies.

Analysis of Response to Therapy for Ulcerative Colitis with OTL0038

Since uptake of OTL0038 was found to predict a response to therapy in arthritic mice, we next investigated whether

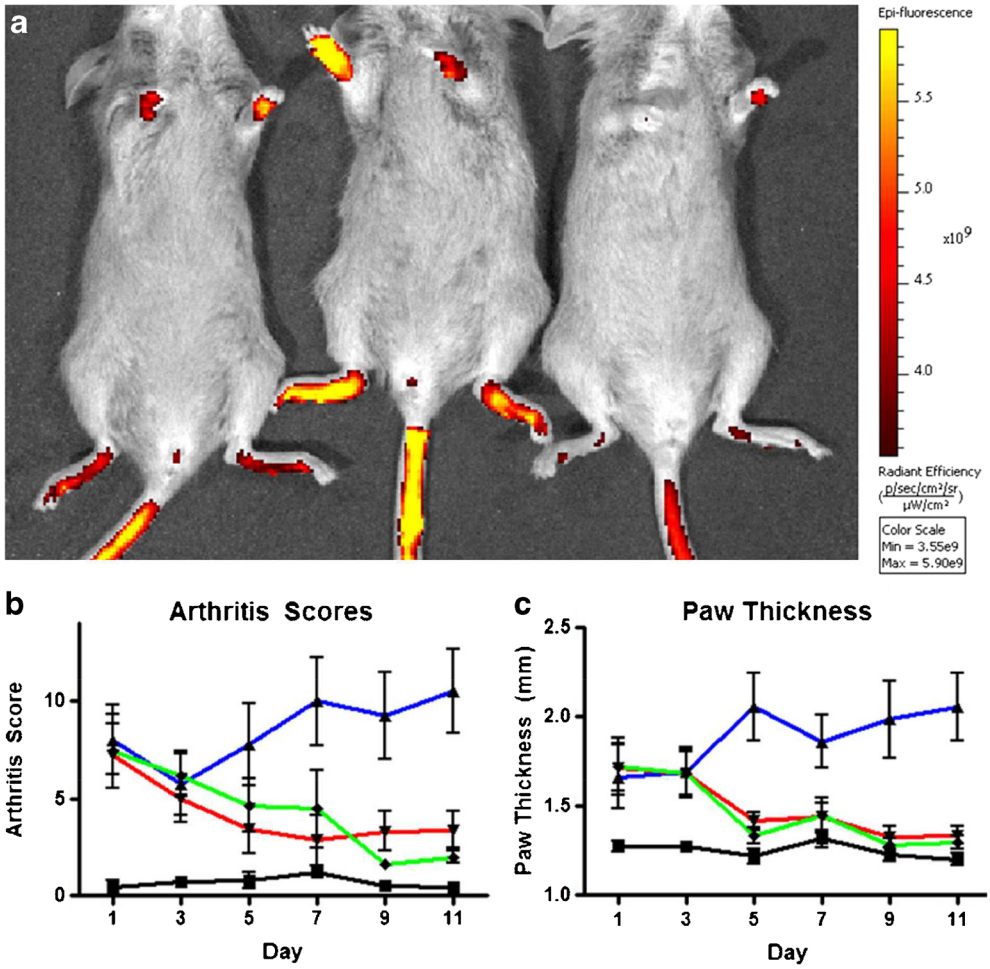

Fig. 1 Analysis of OTL0038 accumulation in CIA mice treated with dexamethasone or abatacept. **a** Overlay of fluorescent on white light image of mice injected with 10 nmol OTL0038 3 days after initiation of treatment with abatacept (*left*), saline (*middle*), or dexamethasone (*right*). OTL0038 uptake is seen in the inflamed appendages and in the tail where the arthritis was induced (see "Methods" section). **b** Arthritis scores and **c** paw thickness measurements of mice ($n=5$) in each of the following treatment groups: disease control (*blue*), abatacept (*red*), dexamethasone (*green*), and healthy control (*black*).

uptake of OTL0038 might be able to similarly predict a response to therapy in a different inflammatory disease model. To explore this hypothesis, mice ($n=10$/group) were administered 5 % dextran sulfate sodium (DSS) in water to induce ulcerative colitis and then treated daily with cimetidine, sulfasalazine, or saline (disease control). On day 4, half of each group was injected with 10 nmol OTL0038 and euthanized in preparation for subsequent imaging of their colons. As seen in Fig. 2a, cimetidine- and sulfasalazine-treated mice showed significantly less OTL0038 uptake in their colons than saline-treated mice, even though there was no significant difference in their clinical scores or colon lengths at this early time point (Fig. 2b, c). More importantly, after 10 days of continuous therapy, treated mice were found to have significantly lower clinical scores and less colon shortening than disease control mice (Fig. 2b, c). And as before, fluorescent images remained essentially unchanged from those collected at the earlier time point (Supplemental Fig. 2). Taken together, these data suggest that imaging with OTL0038 shortly after initiation of therapy can also predict response to treatment in a murine model of inflammatory bowel disease.

Analysis of Response to Therapy for Atherosclerosis with OTL0038

The ability to rapidly predict patient outcomes might be most useful when applied to diseases that are either very slow to progress and respond to therapeutic intervention or unusually difficult to monitor due to their inaccessible locations. Since atherosclerosis suffers from both disadvantages, we next investigated whether OTL0038 might be exploited to predict response to therapy in a common murine model of heart disease. For this purpose, 5-week-old *ApoE−/−* mice were fed a high-fat diet and treated daily with valsartan, fluvastatin, or saline. After 3 weeks of treatment, mice were anesthetized and imaged with OTL0038. As seen in Fig. 3, *ApoE−/−* mice treated with

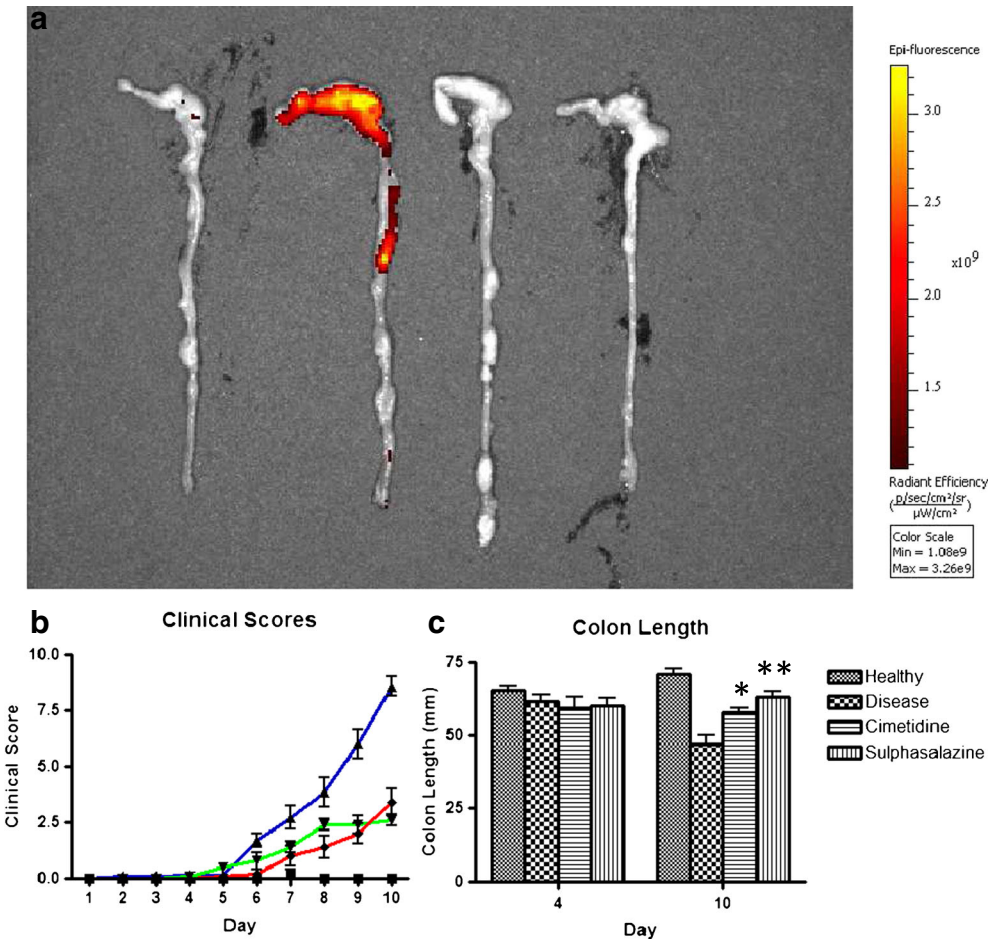

Fig. 2 Analysis of OTL0038 accumulation in colons of mice with ulcerative colitis following treatment with saline, cimetidine, or sulfasalazine. **a** Overlay of fluorescent on white light image of mice injected with 10 nmol OTL0038 4 days after initiation of treatment. From *left* to *right* are colons from healthy control mice, colitis mice treated with saline, colitis mice treated with cimetidine, and colitis mice treated with sulfasalazine. **b** Clinical colitis scores of mice were recorded daily for each treatment group: disease control (*blue*), cimetidine (*red*), sulfasalazine (*green*), and healthy control (*black*). **c** Colons were removed after 4 days of treatment (*left columns*) and 10 days of treatment (*right columns*), and their lengths were measured with calipers. Statistical significance compared to the disease control was determined using a Student's *t* test.*$P \leq 0.05$; **$P \leq 0.01$.

either valsartan or fluvastatin displayed significantly less OTL0038 uptake in their chest cavities than mice treated with saline. As anticipated, fluorescent images at this latter time point revealed a similar pattern of uptake to images obtained following 3 weeks of treatment (Supplemental Fig. 3).

Analysis of Response to Therapy for Pulmonary Fibrosis with OTL0038

Since FR^+-activated macrophages that accumulate in murine models of rheumatoid arthritis and ulcerative colitis are largely composed of classically activated (M1) macrophages [39, 40],

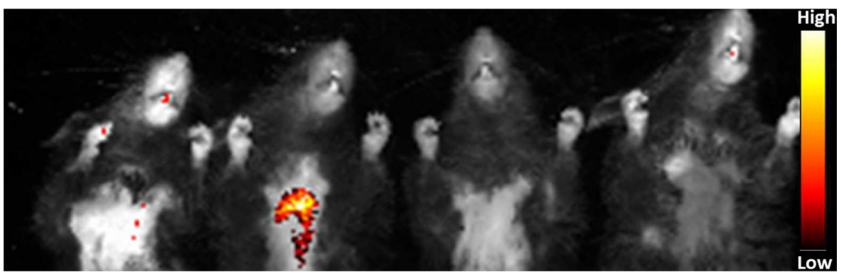

Fig. 3 Analysis of OTL0038 accumulation in the aortic sinuses of *ApoE–/–* mice treated with valsartan or fluvastatin. Overlay of fluorescent on white light image of mice injected with 10 nmol OTL0038 3 weeks after initiation of treatment. From *left* to *right*: healthy (C57BL/6) mouse, *ApoE–/–* mouse treated with saline, *ApoE–/–* mouse treated with valsartan, and *ApoE–/–* mouse treated with fluvastatin.

we decided to explore whether OTL0038 imaging might also prove useful in predicting response to therapy in autoimmune diseases that are predominantly driven by alternatively activated (M2) macrophages. Because pulmonary fibrosis is reported to be mediated by M2 macrophages [41], C57BL/6 mice were induced to develop an acute form of lung fibrosis by intratracheal instillation of bleomycin. Following disease induction, mice were treated daily with dexamethasone, etanercept, or saline and then imaged with OTL0038 after 6 days. As shown in Fig. 4a, dexamethasone- and etanercept-treated mice showed less accumulation of OTL0038 than saline-treated disease control mice. Moreover, on day 15 of treatment, when mice were again imaged with OTL0038 (Supplemental Fig. 4), dexamethasone- and etanercept-treated mice displayed decreased total cell counts in their bronchoalveolar lavage fluids, as well as reduced hydroxyproline contents in their resected lung tissues compared to saline-treated disease controls (Fig. 4b, c). H&E analysis of the lungs also confirmed the reduced fibrosis in mice treated with dexamethasone or etanercept (Fig. 4d). Taken together, these data indicate that OTL0038 imaging can predict response to treatment in an inflammatory disease mediated by alternatively activated (M2) macrophages.

Discussion

In this exploratory study, we demonstrate that OTL0038, a folate receptor-targeted near-infrared (NIR) imaging agent, can accurately predict response to therapy before clinical changes are observed in murine models of rheumatoid

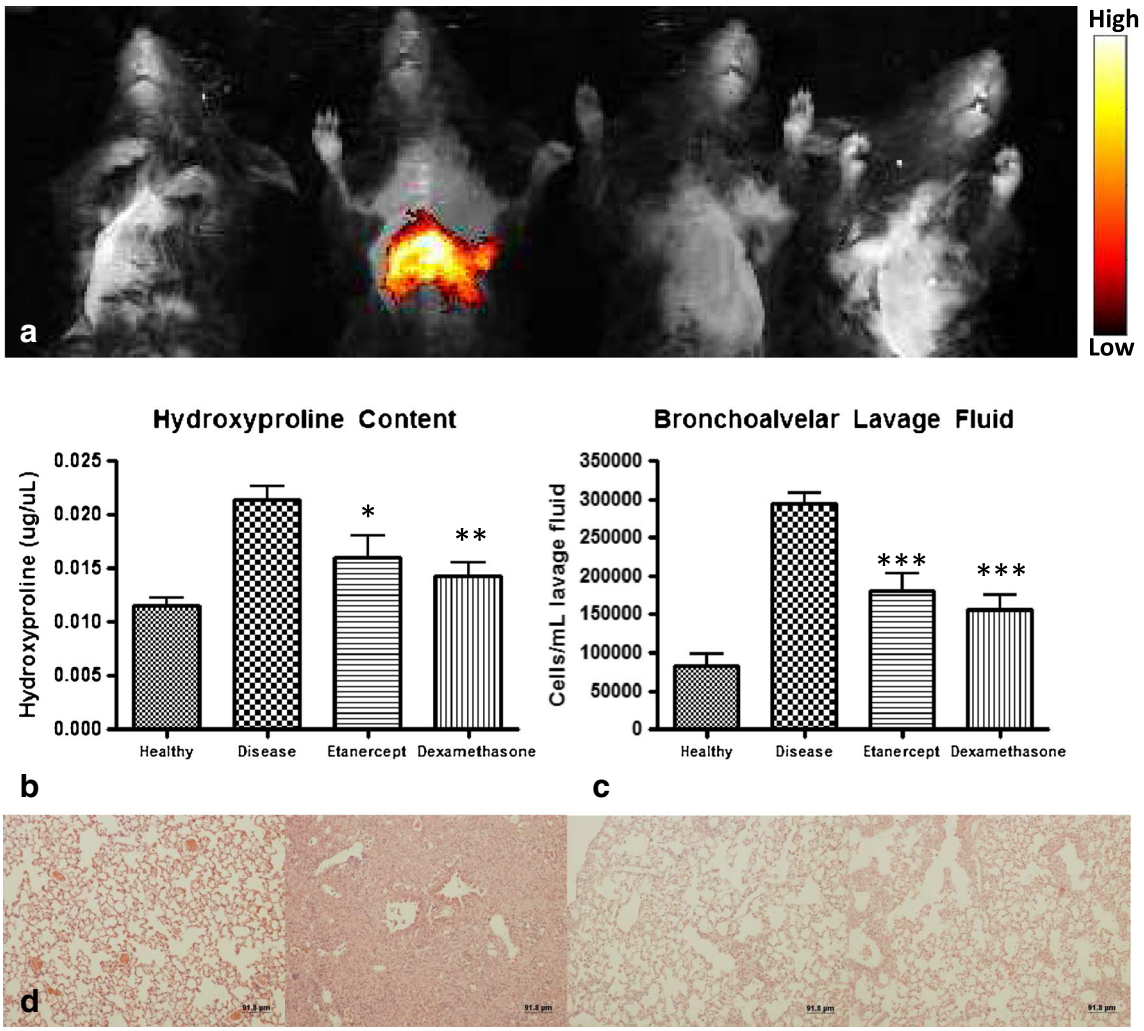

Fig. 4 Analysis of OTL0038 accumulation in mice with pulmonary fibrosis treated with etanercept or dexamethasone. **a** Overlay of representative fluorescent on white light image of mice injected with 10 nmol OTL0038 6 days after initiation of treatment. From *left* to *right*, healthy control mouse, mouse treated with saline, mouse treated with dexamethasone, and mouse treated with etanercept. **b** Hydroxyproline content of lungs measured after 15 days of daily treatment. **c** Total cell count of the bronchoalveolar lavage fluid after 15 days of treatment. **d** Representative H&E stains of lung tissues resected from each treatment group (from *left* to *right*): healthy control mouse, mouse treated with saline, mouse treated with dexamethasone, and mouse treated with etanercept. Statistical significance compared to the disease control was determined using a Student's *t* test $^{*}P \leq 0.05$; $^{**}P \leq 0.01$; $^{***}P \leq 0.001$.

arthritis, ulcerative colitis, atherosclerosis, and pulmonary fibrosis. While uptake of folate receptor-targeted fluorescent dyes has been previously reported to reveal sites of inflammation [21, 24, 42], this paper constitutes the first report showing a correlation between early changes in folate receptor-targeted dye uptake and clinical disease activity at the end of therapy. Assuming that these results can be translated to related human pathologies, the methodology could find application in selecting an optimal therapy for management of human autoimmune/inflammatory diseases.

Folate receptor-targeted radioimaging agents have proven similarly useful for imaging sites of inflammation in both humans and animal models of human inflammatory diseases [20–23]. While folate-targeted radioimaging methods may allow visualization of inflamed lesions that reside deeper within an affected patient, fluorescence imaging with an NIR dye may be preferred when the inflamed tissue is located near a body surface. Thus, because of its benign nature, repeated imaging of the same patient might be possible with a fluorescent dye where it would be discouraged with a radioactive probe. With the aid of an appropriate camera, fluorescence imaging might also be used to guide real-time localized therapy/surgery of an inflamed lesion, where a radioactive reporter would be mechanistically inadequate. Such localized interventions could include direct drug injection (*e.g.*, arthritic joint), surgical resection of the inflamed tissue (*e.g.*, ulcerative colitis), or implantation of a stent (*e.g.*, atherosclerosis) or other interventional device.

Conclusions

OTL0038 has been shown to localize at sites of inflammation in murine models of human autoimmune/inflammatory disease and allow prediction of response to therapies for rheumatoid arthritis, ulcerative colitis, atherosclerosis, and pulmonary fibrosis. Translation of this predictive capability to humans could reduce both the progressive tissue damage and unnecessary expenses associated with use of an ineffective drug in the clinic.

Acknowledgments. This work was supported by a research grant from On Target Laboratories, LLC.

Conflict of Interest. PSL is a board member, significant shareholder, and Chief Science Officer of On Target Laboratories LLC, which was incorporated in 2010. All other authors declare no competing interests.

Authors' contributions. LEK designed the study, performed the experiments, analyzed the data, and wrote the manuscript. SM synthesized the OTL0038. PSL conceived and supervised the study as well as reviewed the manuscript.

References

1. Bennett AN, Peterson P, Zain A et al (2005) Adalimumab in clinical practice: outcome in 70 rheumatoid arthritis patients, including comparison of patients with and without previous anti-TNF exposure. Rheumatology 44:1026–1031
2. Bazzani C, Filippini M, Caporali R et al (2009) Anti-TNF α therapy in a cohort of rheumatoid arthritis patients: clinical outcomes. Autoimmun Rev 8:260–265
3. Rau R (2005) Have traditional DMARDs had their day? Effectiveness of parenteral gold compared to biologic agents. Clin Rheumatol 24:189–202
4. Yazici Y (2007) Monitoring response to treatment in rheumatoid arthritis. Which tool is best suited for routine "real world" care? Bull NYU Hosp Jt Dis 65(Suppl 1):S25–S28
5. Ory PA (2003) Interpreting radiographic data in rheumatoid arthritis. Ann Rheum Dis 62:597–604
6. Taylor PC (2003) The value of sensitive imaging modalities in rheumatoid arthritis. Arthritis Res Ther 5:210–213
7. (1996) American College of Rheumatology Ad Hoc Committee on Clinical Guidelines. Guidelines for the management of rheumatoid arthritis. Arthritis Rheum 37:713–722
8. Breedveld FC (2003) Should rheumatoid arthritis be treated conservatively or aggressively? Rheumatology 42:ii41–ii43
9. Lard LR, Visser H, Speyer I et al (2001) Early versus delayed treatment in patients with recent-onset rheumatoid arthritis: comparison of two cohorts who received different treatment strategies. Am J Med 111:446–451
10. Tsakonas E, Fitzgerald AA, Fitzcharle MA (2000) Consequences of delayed therapy with second line agents in rheumatoid arthritis: a 3 year followup on the hydroxychloroquine in early rheumatoid arthritis (HERA) study. J Rheumatol 27:623–629
11. Escobedo JO, Rusin O, Lim S (2010) Strongin RM (2010) NIR dyes for bioimaging applications. Curr Opin Chem Biol 14:64
12. Kitai T, Inomoto T, Miwa M, Shikayama T (2005) Fluorescence navigation with indocyanine green for detecting sentinel lymph nodes in breast cancer. Breast Cancer 12:211–215
13. Werner SG, Langer HE, Schott P et al (2013) Backhaus M: indocyanine green-enhanced fluorescence optical imaging in patients with early and very early arthritis: a comparative study with magnetic resonance imaging. Arthritis Rheum 2013(65):3036–3044
14. Werner SG, Langer HE, Ohrndorf S et al (2012) Inflammation assessment in patients with arthritis using a novel in vivo fluorescence optical imaging technology. Ann Rheum Dis 71:504–510
15. Okochi O, Kaneko T, Sugimoto H et al (2002) ICG pulse spectrophotometry for perioperative liver function in hepatectomy. J Surg Res 103:109–113
16. Tanaka E, Chen FY, Flaumenhaft R et al (2009) Real-time assessment of cardiac perfusion, coronary angiography, and acute intravascular thrombi using dual-channel near-infrared fluorescence imaging. J Thorac Cardiovasc Surg 138:133–140
17. Chang AA, Morse LS, Handa JT et al (1998) Histologic localization of indocyanine green dye in aging primate and human ocular tissues with clinical angiographic correlation. Ophthalmology 105:1060–1068
18. Nakashima-Matsushita N, Homma T, Yu S (1999) Selective expression of folate receptor beta and its possible role in methotrexate transport in synovial macrophages from patients with rheumatoid arthritis. Arthritis Rheum 42:1609–1616
19. Xia W, Hilgenbrink AR, Matteson EL et al (2009) A functional folate receptor is induced during macrophage activation and can be used to target drugs to activated macrophages. Blood 113:438–446
20. Paulos CM, Varghese B, Widmer WR et al (2006) Folate-targeted immunotherapy effectively treats established adjuvant and collagen-induced arthritis. Arthritis Res Ther 8:R77
21. Vaitilingam B, Chelvam V, Kularatne SA et al (2012) A folate receptor-α-specific ligand that targets cancer tissue and not sites of inflammation. J Nucl Med 53:1127–1134
22. Turk MJ, Breur GJ, Widmer WR et al (2002) Folate-targeted imaging of activated macrophages in rats with adjuvant-induced arthritis. Arthritis Rheum 46:1947–1955
23. Matteson EL, Lowe VJ, Prendergast FG (2009) Assessment of disease activity in rheumatoid arthritis using a novel folate targeted radiopharmaceutical Folatescan. Clin Exp Rheumatol 27:253–259
24. Jager NA, Westra J, van Dam GM (2012) Targeted folate receptor β fluorescence imaging as a measure of inflammation to estimate vulnerability within human atherosclerotic carotid plaque. J Nucl Med 2012(53):1222–1229
25. Hansen MJ, Low PS (2011) Folate receptor positive macrophages: cellular targets for imaging and therapy of inflammatory and autoimmune diseases. In: Jackman AL, Leamon CP (eds) Targeted drug strategies for cancer and inflammation. Springer, New York, pp 181–193

26. Mahalingam SM, Kularatne SA, Roy J, Low PS (2013) Evaluation of pteroyl-amino acid-NIR dye conjugates for tumor targeted fluorescence guided surgery. [abstract]. Papers of the American Chemical Society 246 MEDI 329
27. Gagare PD, Noshi M, Myers C, Kularatne SA, Low PS: OTL-0038 (2013) A potent folate receptor (FR)-targeted NIR dye. [abstract]. Papers of the American Chemical Society 246 MEDI 328
28. Brand DD, Latham KA, Rosloniec EF (2007) Collagen-induced arthritis. Nat Protoc 2:1269–1275
29. Inglis JJ, Criado G, Medghalchi M (2007) Collagen-induced arthritis in C57BL/6 mice is associated with a robust and sustained T-cell response to type II collagen. Arthritis Res Ther 9:R113
30. Webb LM, Walmsley MJ, Feldmann M (1996) Prevention and amelioration of collagen-induced arthritis by blockade of the CD28 co-stimulatory pathway: requirement for both B7-1 and B7-2. Eur J Immunol 26:2320–2328
31. Wirtz S, Neufert C, Weigmann B, Neurath MF (2007) Chemically induced mouse models of intestinal inflammation. Nat Protoc 2:541–546
32. Smith JA (1983) The effect of atropine, cimetidine and FPL 52694 on duodenal ulcers in mice. Eur J Pharmacol 88:215–221
33. Axelsson LG, Landstrom E, Bylund-Fellenius AC (1998) Experimental colitis induced by dextran sulphate sodium in mice: beneficial effects of sulphasalazine and olsalazine. Aliment Pharmacol Ther 12:925–934
34. Zadelaar S, Kleemann R, Verschuren L et al (2007) Mouse models for atherosclerosis and pharmaceutical modifiers. Arterioscler Thromb Vasc Biol 27:1706–1721
35. Iwashita M, Nakatsu Y, Sakoda H et al (2013) Valsartan restores inflammatory response by macrophages in adipose and hepatic tissues of LPS-infused mice. Adipocyte 2:28–32
36. Li Z, Iwai M, Wu L et al (2004) Fluvastatin enhances the inhibitory effects of a selective AT1 receptor blocker, valsartan, on atherosclerosis. Hypertension 44:758–763
37. Moore BB, Hogaboam CM (2008) Murine models of pulmonary fibrosis. Am J Physiol Lung Cell Mol Physiol 294:L152–160
38. Moeller A, Ask K, Warburton D et al (2008) The bleomycin animal model; a useful tool to investigate treatment options for idiopathic pulmonary fibrosis? Int J Biochem Cell Biol 40:362–382
39. Kinne RW, Bräuer R, Stuhlmüller B et al (2000) Macrophages in rheumatoid arthritis. Arthritis Res 2:189–202
40. Hunter MM, Wang A, Parhar KS et al (2010) In vitro-derived alternatively activated macrophages reduce colonic inflammation in mice. Gastroenterology 138:1395–1405
41. Pechkovsky DV, Prasse A, Kollert F et al (2010) Alternatively activated alveolar macrophages in pulmonary fibrosis-mediator production and intracellular signal transduction. Clin Immunol 137:89–101
42. Chen WT, Mahmood U, Weissleder R, Tung CH (2005) Arthritis imaging using a near-infrared fluorescence folate-targeted probe. Arthritis Res Ther 7:R310–R317